Cavitation in thermoplastic melts: New insights into ultrasound-assisted fibre-impregnation

Iakovos Tzanakis [a,b,*], Mohammad Khavari [a,b], Maik Titze [c], Dmitry G. Eskin [d,**]

[a] *Faculty of Technology, Design and Environment, Oxford Brookes University, Oxford, OX33 1HX, UK*
[b] *Department of Materials, University of Oxford, Oxford, OX1 3PH, UK*
[c] *German Aerospace Centre, Institute of Composite Structures and Adaptive Systems, Lilienthalplatz 7, 38108, Braunschweig, Germany*
[d] *Brunel University London, Brunel Centre for Advanced Solidification Technology, Uxbridge, UB8 3PH, UK*

ARTICLE INFO

ABSTRACT

The impregnation of continuous carbon fibre roving with thermoplastic melt is a challenging task due to the high viscosity and surface tension of the melt. A new technique is under development utilizing ultrasonic oscillations within the thermoplastic melt which encloses a fibre roving, to achieve fibre impregnation. Despite ultrasonic processing being very efficient, the specific conditions created in the thermoplastic melt have never been studied before. This study investigated whether cavitation effects could be present during ultrasound-assisted fibre impregnation. The observed acoustic effects allowed us to suggest the possible underlying mechanisms. For the purpose of the study a melt-bath impregnation setup with polylactide was built. To detect the cavitation effects and acoustic parameters a calibrated high-temperature cavitometer was used. The results showed the formation of small cavitation zones in the direct vicinity to the sonotrode tip where the fibre roving would be positioned. Therefore, the occurrence of cavitation was established, and induced effects like shock waves, microjets and microstreaming should be further considered for detailed investigation of the ultrasound-assisted impregnation mechanism.

1. Introduction

Thermoplastic composites are receiving more and more attention in industrial applications and particularly in aerospace. In such composite materials, continuous reinforcing elements like carbon fibres are used to significantly increase tensile strength and tensile stiffness in the fibre direction. For a sufficient load transfer, the impregnation of these fibres with thermoplastic matrix material as well as the fibre-matrix bonding quality are of particular importance. The reinforcing fibres are typically available as a roving (bundle of endless single fibre filaments). A 24K carbon fibre roving can be described as continuous fibre bundle with 24,000 single fibre filaments with a typical diameter between 4 and 7 μm. For impregnation, the thermoplastic matrix needs to fully infiltrate the roving by coating each single fibre and bonding the filaments well together. In comparison to duromer resin systems, the viscosity of thermoplastic melt is significantly higher and infiltration requires a lot more effort. Due to this challenging impregnation process, it can be beneficial for part manufacturing to outsource this task to an upstream independent process step by producing pre-impregnated semi-finished products like tapes or filaments. These pre-impregnated materials are then used, e.g., in Automated Fibre Placement or Additive Manufacturing machines, to produce continuous fibre-reinforced thermoplastic parts.

The Institute of Composite Structures and Adaptive Systems of German Aerospace Centre (DLR-FA) investigates in its strategic field of Additive Composite Structures (AddCompS™) how additive manufacturing solutions can create an added value in the design and production of composite components. Especially additive extrusion technologies for 3D-printing with continuous fibre-reinforced materials are of interest. For this technological approach, the availability of affordable continuous fibre-reinforced filaments constitutes a barrier for a wider industrial application. As a possible solution, a new technique is under development enabling direct impregnation of fibre roving with high viscous thermoplastic melt. The working principle is based on the introduction of ultrasound using a sonotrode in the thermoplastic melt, which encloses a fibre roving. First results were published recently [1]
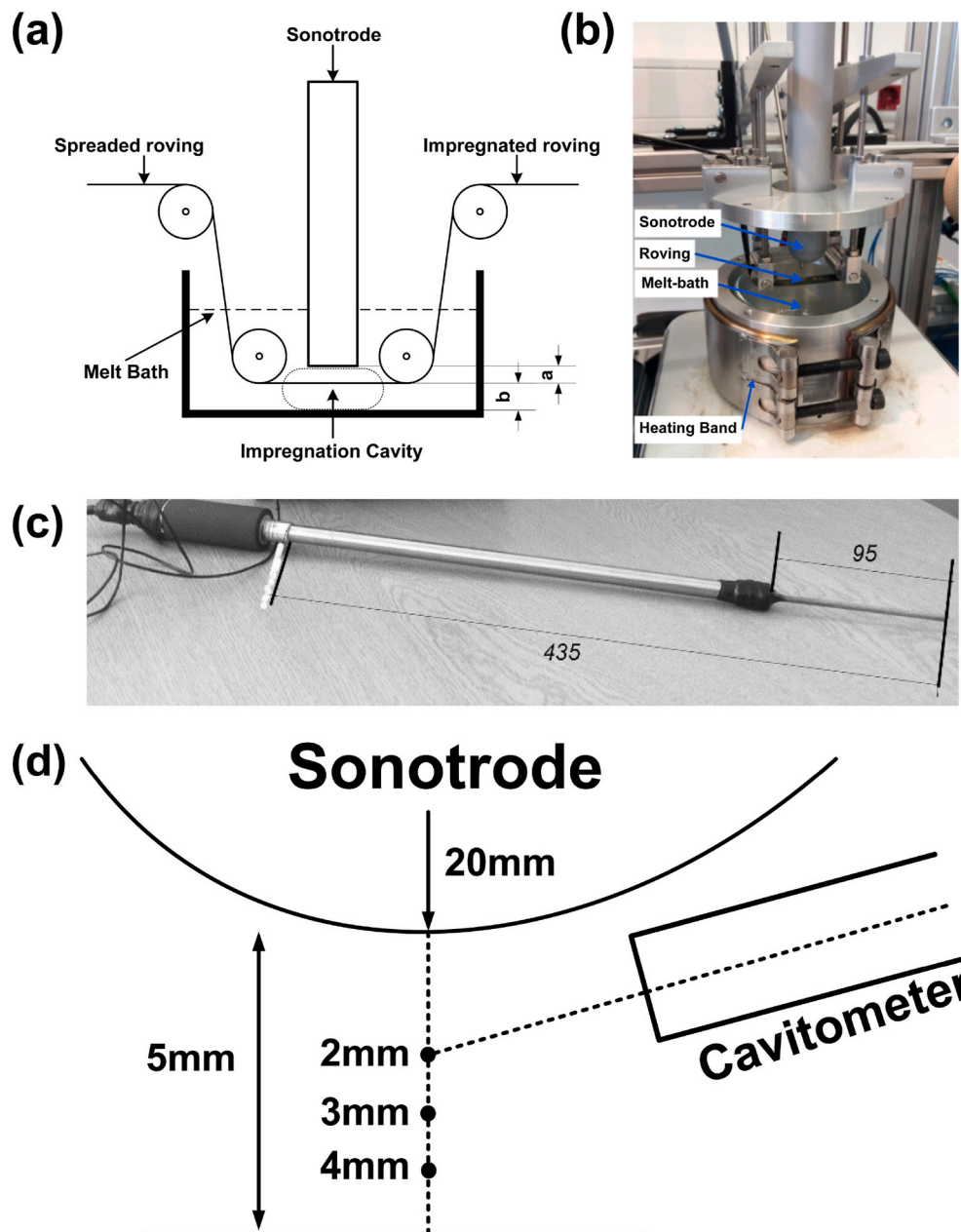

Fig. 1. a) Schematic of the ultrasonic processing melt-bath impregnation setup; b) photograph of the melt-bath impregnation setup; c) high-temperature cavitometer (dimensions are in mm) and d) schematic of the measuring locations.

and reported improved impregnation due to ultrasonic processing.

The use of ultrasound to enhance fibre impregnation has been studied before for applications where the fibres are in direct contact to the sonotrode tip [2–4]. Also ultrasonic processing was suggested for reinforcing metal–matrix of aluminium (Al) [5] or magnesium (Mg) composites [6] as well as improving the impregnation of carbon fibres within an Al–Mg melt [7]. Ultrasound was also applied to a melt bath with thermoplastic resin dissolved in dichloromethane for continuous fibre impregnation as a pre-treatment stage in a 3D-printing process [8]. These investigations revealed the improved impregnation quality and fibre distribution upon ultrasonic processing. Although the effects of ultrasonic parameters such as amplitude on the efficiency of ultrasonic polymer processing have been reported, very little is known on the cavitation induced by ultrasonic oscillations in highly-viscous thermoplastic melts (viscosity at 185 °C is 530 Pa s [9]) upon such processing. Some studies were dedicated to the rheological measurements and

high-speed observations in polymer solutions. The effects of ultrasonic oscillations on the behaviour of non-Newtonian polymer melts are believed to be related to the decrease of the apparent viscosity and changing of the molecular bonds between polymeric chains [10], as a result the cavitation threshold becomes a function of the processing time [11]. The high viscosity of polymer melt can significantly alter the dynamics of a cavitation bubble, suppressing its implosion and jet emission as was observed even in aqueous polymer solutions [12,13].

The main hypothesis for the improved performance of the ultrasound-assisted fibre impregnation lies in the cavitation and related phenomena. It can be hypothesised that collapsing cavitation bubbles and acoustic streaming initiate shockwaves and shearing streaming which are responsible for observed fibre impregnation, similar to well-known mechanisms in composite materials and filtration [14]. The cavitation is known to generate acoustic streaming [15,16] that is able to push liquid around the fibres promoting liquid entrainment within the
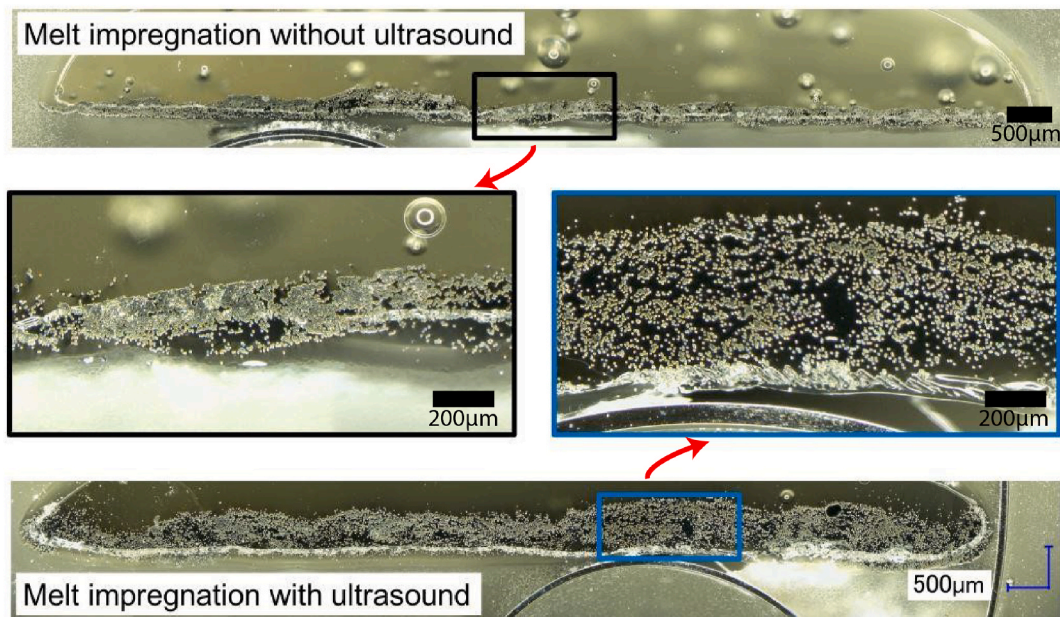
Fig. 2. Cross-section images of impregnated rovings without (first row) and with (third row) introduction of ultrasound into the melt batch. The second row magnifies a certain region of the impregnated melt for both without (left screenshot) and with (right screenshot) ultrasonic treatment. For both rovings, the boundary conditions like melt temperature or residence time in melt are the same.

fibre gaps. In conjunction with the vigorously oscillating bubbles (represented by the multiple ultra-harmonic peaks in the acoustic spectrum) in the vicinity of the fibres, which can push fibres further apart to increase permeability, infiltration of fibre bundle with matrix material can be strongly promoted. This mechanism was recently seen for the exfoliation of graphite to produce graphene [17] where the presence of tiny bubbles in-between graphitic layers promoted their opening during the rarefaction phase. Additionally, the quality of fibre to polymer matrix bonding should be improved due to better wetting of these fibres due to the sonocapillary effect [18]. In the case of collapsing cavitation bubbles in the immediate vicinity of a spatial boundary such as a fibre bundle, directed microjets as well as transient local pressure fluctuations due to shock waves should occur. These would additionally promote penetration of the fluid into the fibre bundle.

To better understand underlying mechanisms of the ultrasound-assisted fibre impregnation technique, it is important to detect the cavitation phenomenon during ultrasound treatment. As has been mentioned above, this phenomenon had not been well studied in highly viscous media like thermoplastic melts. Without this direct evidence the hypotheses outlined above cannot be substantiated.

Our research teams in Oxford Brookes and Brunel Universities have extensively studied cavitation effects occurring during ultrasound processing of low and high temperature (up to 800 °C) liquids using state-of-the-art hydrophones and cavitometers [19–21]. In the previous work a high-temperature cavitometer was used with appropriate procedures of calibration and signal processing, allowing one to acquire an acoustic spectrum as well as convert the measured data into acoustic pressure [21–23].

Therefore, within this study a melt-bath laboratory setup integrated with a high-temperature cavitometer was deployed to study the cavitation effects during ultrasound-assisted fibre-impregnation. The base setup, where a 24K carbon fibre roving was spread and placed in molten thermoplastic polylactide (PLA) melt underneath a sonotrode tip, was described elsewhere [1]. This study is focused on the cavitation phenomenon and does not consider other possible effects of ultrasonication such as polymer degradation, heating and changing of molecular structure, which are considered negligible taking into account a short period of processing time (i.e. up to 15 s). In this paper, we firstly summarise the key findings of ultrasound-driven impregnation related to this setup. Afterwards a modification of laboratory setup for cavitation measurement is described. By varying the distance between the cavitometer and sonotrode tips as well as the sonotrode amplitude, the established cavitation field is characterized in the PLA thermoplastic melt and water (for comparison). The resulting frequency spectra and pressure levels are interpreted in terms of cavitation development and correlated to the previously observed impregnation results [1]. Finally, an outlook for continuous industrial processing with promising fibre impregnation and distribution is shown.

2. Experimental setup

The laboratory setup consisted of a glass beaker with an inner diameter of 80 mm and depth of 40 mm as shown in Fig. 1a and b. The glass beaker was placed inside a housing which was heated by a heating band. To prepare the melt bath for the experiments, the glass beaker was filled with PLA granules which were then heated until molten. For all experiments with PLA, the glass beaker was filled about 75% with the thermoplastic melt. The melt temperature was precisely (±1 °C) controlled by a thermocouple. To introduce the ultrasound, a ceramic-coated titanium sonotrode attached to a piezoelectric transducer with a rounded half-sphere tip of 20 mm diameter and a driving frequency of 19.5 kHz was immersed into the melt. The half-sphere should be able to concentrate and extent the size of the cavitation zone as in Ref. [24], while the low driving frequency shall promote the generation of powerful collapsing cavitation bubbles. The distance (a+b in Fig. 1a) of the sonotrode tip to the bottom of the glass beaker was 5 mm for all experiments, based on the results of the previous conducted impregnation study [1]. During the experiments, the sonotrode operated in short cycle times, to prevent overheating and degradation of the melt. As a short distance between the sonotrode tip to the fibre roving was previously shown to be essential for achieving good impregnation results, the acoustic field in the direct vicinity to the sonotrode tip was characterized. For that purpose, an advanced calibrated high-temperature cavitometer as shown in Fig. 1c and described in detail elsewhere [22] was placed in the area of interest at an angle of 45° allowing its movement in the melt (Fig. 1d). During these experiments no fibre roving was present

Table 1
Parameter settings for cavitation measurements.

No.	Liquid	Transducer amplitude %	Vertical distance between the sonotrode tip and the cavitometer (mm)
1	Water	50%	2
2	PLA	50%	2
3	PLA	50%	3
4	PLA	50%	4
5	Water	100%	2
6	PLA	100%	2
7	PLA	100%	3
8	PLA	100%	4

due to the limited space. The raw digital output from the cavitometer (in mV) as acquired by an attached external digital oscilloscope device PicoScope-3204D (Pico Technology). The PicoScope allowed real-time signal monitoring of the cavitometer sensor's data and ultrasonic parameters. A Blackman window was applied to the raw voltage signal that was then transformed to the frequency domain via Fast Fourier Transform. Unless otherwise specified, average of 60 acquired signals were typically taken using a resolution bandwidth of 762.9 Hz. The time for this signals acquisition was approximately 300 ms. Each experiment was repeated three times to ensure the reproducibility of results. The details of the calibration procedure, signal processing and extracting spectral information and pressure values can be found elsewhere [22,23]. Similar experiments were performed with water with the same settings,

except for the temperature, as water experiments were conducted at room temperature. This allows to compare the results of PLA to those of water, for which generation and characterization of cavitation effects are well understood.

In order to characterise the cavitation behaviour, the sonotrode amplitude as well as the position of the cavitometer in relation to the sonotrode tip were varied as shown in Fig. 1d. Table 1 shows the used parameter settings.

For the PLA material, the melt temperature was set to 180 °C. The transducer input power was in the range of 25–62 W with peaks up to 100 W. As described in Ref. [1], the sonotrode tended to decouple from the melt due to the bad acoustic impedance matching. This decoupling already started after about 4 s of treatment time. Therefore, only short operation cycles were used to capture the data. The positioning of the cavitometer was carried out by manual movement at fixed locations. As the overall distance of the sonotrode tip to the bottom of the glass beaker was fixed at 5 mm, the possibility for an appropriate precise manual positioning was assumed. In all cases, the cavitometer was tilted allowing to place its tip as close as possible to the central axis of the sonotrode, while avoiding direct contact of the cavitometer to boundary elements. In that way, the cavitation field in the direct vicinity to the sonotrode tip could be analysed. The vertical distance of sonotrode tip to centreline of the cavitometer tip as well as the sonotrode amplitude were varied as shown in Table 1.
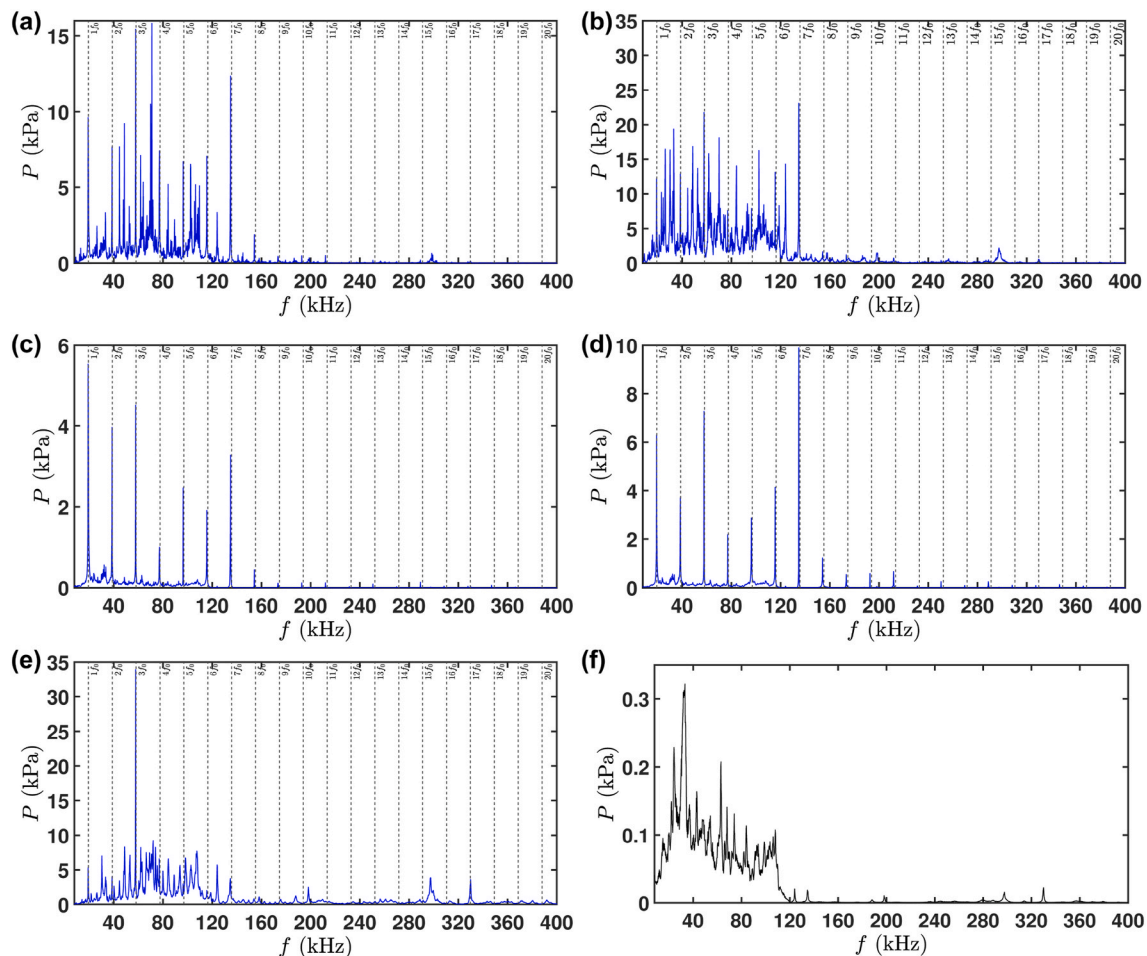

Fig. 3. Acoustic spectrum a) in liquid PLA at 50% input power, captured with cavitometer 2 mm from the tip of the sonotrode; b) in liquid PLA at 100% input power at 2 mm; c) in liquid PLA at 50% input power at 4 mm; d) in liquid PLA at 100% input power at 4 mm and e) in water at 100% input power. Driving frequency (f_0) is 19.5 kHz. f) Background noise with the tip of the cavitometer submerged inside the liquid PLA and all the electronics turned on (no sonication at this step). Note the different scales of Y-axis.
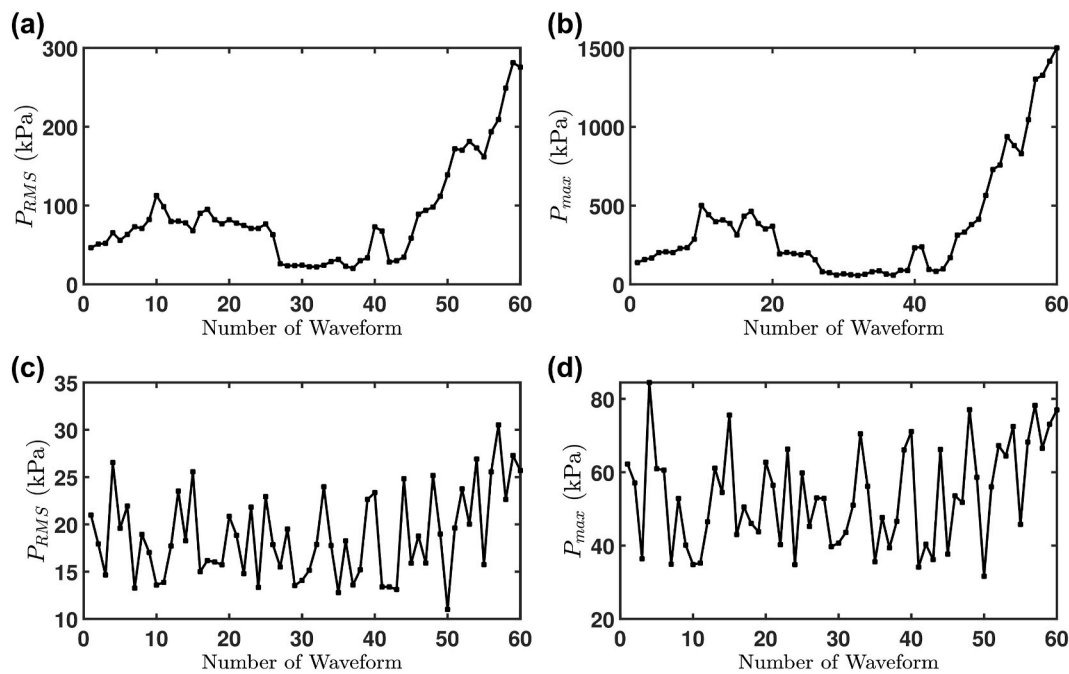
Fig. 4. The measured acoustic pressures for each 60 waveforms of 5 ms each in PLA melt at 50% power and at 2 mm (a, b) and 4 mm from the sonotrode tip (c, d): (a, c) the RMS pressure and (b, d) the maximum pressure.

3. Results and discussion

3.1. Preliminary results on ultrasound-assisted fibre impregnation

The preliminary study on direct melt bath impregnation with PLA material utilizing ultrasound was reported elsewhere [1] and due to limited space, it has been conducted without cavitometer as explained in Section 1. Basic findings of this study as well as the working principle of the new developed ultrasound-assisted fibre impregnation technique of DLR-FA as shown in Fig. 1a and b are described below.

The ultrasound-assisted technique for fibre-impregnation was based on the introduction of ultrasound into thermoplastic melt which enclosed a fibre roving. The ultrasound was, therefore, not used to melt the material nor was the sonotrode in direct contact with the fibre roving. For basic evaluation of suitable process design, a melt bath laboratory setup was built as shown in Fig. 1a. A fibre roving was spread by a simple roller mechanism (see Fig. 1a and b) and placed underneath the sonotrode tip inside thermoplastic melt. The roving was treated for time periods of 3–15 s with ultrasound while statically remaining in its position. Afterwards the roving was pulled out and cut at the treatment position to capture ultrasound effect using cross-section images. A study varying the distance a from −1 mm (direct contact) to 4 mm and distance b from 1 mm to 9 mm showed that the distance a between sonotrode tip and fibre roving needed to be low but direct contact to roving should be prevented [1]. Already after 3 s of treatment, a significant influence on fibre impregnation and fibre distribution due to ultrasound could be observed in comparison to a roving passing the melt bath without ultrasonic treatment as illustrated in Fig. 2. It needs to be mentioned that the introducible power starts to decrease after 4 s treatment time due to decoupling of the sonotrode tip to the melt, as shown earlier in Section 2. Fibres in the case of the untreated roving were found to form clusters of dry fibres resulting in a thin layer with an average height of 0.23 mm. In the case of insonicated melt, the fibres were spread nicely, forming a thick boundary (0.63 mm average) approximately 3 times larger, indicating the deagglomeration and dispersion efficacy of ultrasound. Next step was to understand the role cavitation played in this process by checking the acoustic spectrum for each of the studied cases of Table 1.

3.2. Acoustic pressure measurements and spectrum analysis

The cavitation activity in the highly viscous PLA liquid was captured using an advanced high-temperature calibrated cavitometer. Initially the background noise was captured without switching on the ultrasound (Fig. 3f), which was later subtracted in the frequency domain for all the processed cases. As one can see the background noise caused by the electric/electronic emissions is rather small and not related to any regular oscillations.

The analysis of the captured cavitation emissions and corresponding spectra in PLA melt at both input power settings showed evidence of developed cavitation zone only in the close proximity to the sonication tip, i.e. only in the case where the cavitometer was placed at a distance of 2 mm from the sonotrode tip, as demonstrated by well-defined cavitation spectra in Fig. 3a and b. Here one can observe harmonics, subharmonics and ultra-harmonics along with the broadband noise. There was an obvious peak at the fundamental frequency at 19.5 kHz and the corresponding harmonics (up to the 8th harmonic) related to the direct driving field, with further contributions from linear/volumetric bubble oscillations. The rise of the broadband noise and the appearance of numerous prominent ultra-harmonic peaks as well as small subharmonic peaks indicated an established acoustic cavitation regime. Specifically, broadband noise is regarded as a product of shock waves emissions from non-spherical and vigorously oscillating/collapsing cavitation bubbles (transient cavitation) while ultra- and sub-harmonics are associated with nonlinear volumetric and surface oscillation (stable cavitation) of the cavitation bubbles [25]. It has been shown that prominent subharmonic peaks are also associated with shock wave emissions from collapsing bubbles or bubbly clusters [26]. These acoustic signatures represented the intensity of cavitation. Note that the broadband noise level as well as the pressure increased significantly with the increased input power. In the cases of measurements 3 mm and 4 mm away from the sonotrode tip, a non-cavitating spectrum was captured with prominent harmonic peaks of the fundamental frequency at multiple integers, but no broadband noise and subharmonics typical of cavitation (see Fig. 3c and d). Note that only the 4 mm case is shown as the 3 mm case was similar.

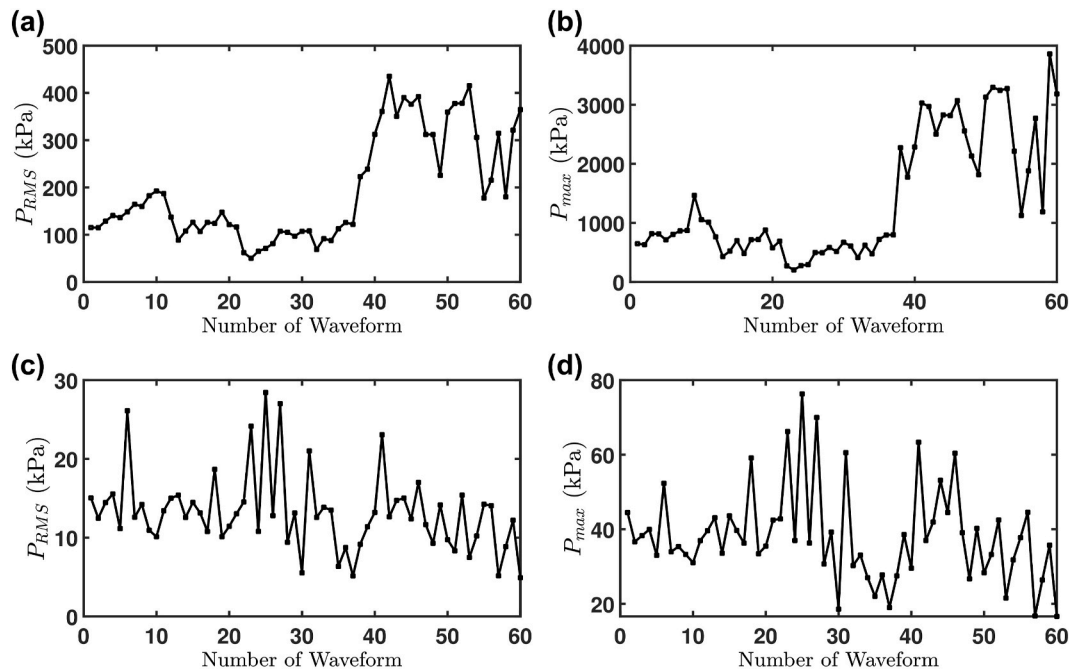Fig. 4 shows the root-mean-square (RMS) P_{RMS} and maximum (P_{max})

Fig. 5. The measured acoustic pressures for each 60 waveforms of 5 ms each in PLA melt at 100% power and at 2 mm (a, b) and 4 mm from the sonotrode tip (c, d): (a, c) the RMS pressure and (b, d) the maximum pressure.

pressures averaged across 60 captured waveforms of 5 ms period each for the case of 50% power and for two distances (2 and 4 mm) from the ultrasonic source. The RMS pressures from the 2 mm case were in the range of 30–250 kPa (Fig. 4a) while the peak values reached 1500 kPa (Fig. 4b). It is worth noting that the pressures in the vicinity of the sonotrode increased with the acquisition time (even it was quite short, 300 ms), which might indicate the development of more active cavitation as the viscosity was lowered by the acoustic streaming and better coupling was achieved. Similar trend has been observed in the case of 100% power (Fig. 5a and b) while the pressure values almost doubled. In contrast, the acoustic pressures, both RMS and maximum, were significantly lower at a 4 mm distance and did not show systematic variation with the time of measurement nor with the increase in input power (Fig. 4 c,d and Fig. 5 c,d). This demonstrated the great capacity of PLA liquid to absorb acoustic emissions and restrict their propagation in the bulk liquid, resulting in a very confined cavitation zone. This has been previously seen in glycerol (another highly viscous liquid) but to a lesser extend [19]. The cavitation zone within this highly viscous thermoplastic material seemed to extent at a radial distance to around 2 mm from the tip sonotrode and then decayed rapidly. Specifically, in the case of 50% input power (Fig. 4) the RMS pressure decay was in the range of 60–90% as the sensor departs from the 2 mm to 4 mm distances, while for the case of 100% (Fig. 5) this decay was 85–93%.

The pressure magnitude in the case of 100% at 2 mm was higher than the corresponding 50% case with averaged RMS pressure values reaching 400 kPa (Fig. 5a) and the maximum reaching up to 3.5 MPa (Fig. 5b). This means that shielding of the acoustic field by the cavitation zone did not play significant role in PLA melt, unlike water where the increase of the input power frequently led to the drop of acoustic pressure [27]. On the other hand, the cavitation zone is much more confined in the PLA melt than in water, which is due to the much more significant attenuation caused by the high viscosity and non-Newtonian nature of the thermoplastic melt. Apparently, in the PLA melt, due to the highly viscous nature of the liquid, a significant amount of input power is needed to initiate and maintain the cavitation even though it occurs in a much limited space, which partially agrees with the conclusions of [11].

Another indication of the strong cavitation activity within this 2 mm region is a direct comparison of the acoustic spectrum in PLA with that

Table 2
Averaged RMS and maximum pressure values from 60 waveforms of 5 ms each (STD is the standard deviation).

Case	P_{max} (kPa)	STD_{Pmax} (kPa)	P_{RMS} (kPa)	STD_{PRMS} (kPa)
50% Water (2 mm)	560	157	140	35
50% PLA (2 mm)	365	362	86	63
50% PLA (3 mm)	67	24	23	6
50% PLA (4 mm)	54	14	19	4.5
100% Water (2 mm)	510	89	126	19
100% PLA (2 mm)	1390	1050	195	112
100% PLA (3 mm)	47	17	17	6
100% PLA (4 mm)	77	15	27	6

of water where cavitation was apparent and visible, using the same cavitometer device. By comparing Fig. 3b and e (only treatment at 100% input power is shown) it can be deduced that water and PLA at 2 mm shared a similar acoustic spectrum pattern, which of course differs significantly from the other studied cases of 3- and 4-mm distances. Furthermore, it is interesting to note that in the 2-mm PLA case, peaks at higher frequencies (>100 kHz) are more prominent as compared to water, implying the existence of smaller cavitating bubbles, resonating for significant periods of time. This is something that has been also previously noticed in cavitation experiments within highly viscous fluids such as glycerine where bubbly structures were sustained for significant periods of time [19]. Interestingly and in contrast to PLA where prominent peaks beyond the fundamental frequency were present in frequencies such as $3f_0$, $3/4f_0$, $7f_0$ and up to 140 kHz ($8f_0$) (associated with the resonance mode of various bubbles sizes confined within the supressed cavitation zone); in water there was only one prominent peak associated with the 3rd harmonic. This indicates a resonance mode that may be attributed to 1) the size and dimensions of the vessel as previously seen in Ref. [26] (the sides of the sonotrode are in approximately distance of ~30 mm from the sides of the glass beaker that coincides with the wavelength of the 60 (3×20) kHz in water and should promote the formation of standing waves); 2) the majority of the vigorously oscillating bubbles fall to sizes close to 50 μm (associated with a 60 kHz
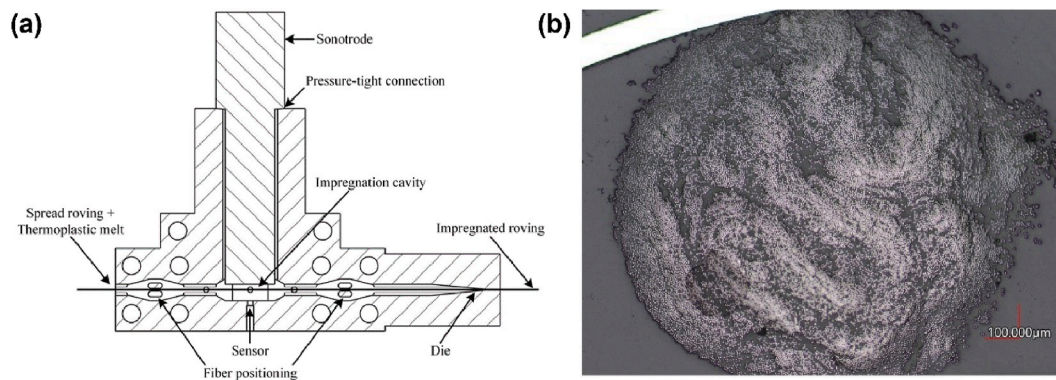
Fig. 6. Extrusion tool for continuous ultrasound-assisted fibre impregnation (a) and produced 3D-printing filament from PLA (b).

resonance mode); 3) the harmonic cascading as explained in Ref. [28]; or 4) the non-linearity parameter of the host medium (water) that promotes waveform distortions of that frequency.

The averaged RMS and maximum pressure values corresponding to the studied positions in the PLA melt as well as in water are given in Table 2. These results support our analysis (Figs. 4 and 5) of attenuation and shielding phenomena in PLA and water. In particular, pressure values in water were similar for both input powers primarily due to acoustic shielding, while in PLA the pressure increased about 4 times with input power doubling. On the other hand, in the PLA the developed pressure was pronounced only at 2 mm where cavitation was sustained prior to being significantly decayed due to the highly viscous environment. It can be noticed that only in the case of the 2 mm distance, the acoustic pressure in PLA was significant and about 60% higher (for the 100% power case) than that of water unlike all other cases where the acoustic pressure was significantly lower and related with the pressure build up only by the fundamental frequency emissions. Also, the large error values are an indication of the very viscous nature of the PLA with coupling and decoupling phenomena occurring in due time, promoting (coupling) or suppressing (de-coupling) cavitation activity near the sonotrode. However, it is obvious that when the cavitation activity was developed, the acoustic pressure surges (P_{max}) were very powerful reaching MPa range.

We can, therefore, conclude that the cavitation phenomena do occur upon ultrasonic processing of PLA, being confined to the vicinity of the ultrasonic source where the impregnation of carbon-fibre roving effectively happens.

4. Design of continuous ultrasound-assisted fibre impregnation tool

Based on the acoustic studies, the technique of ultrasonic impregnation was transferred to an extrusion tool for continuous operation. A schematic representation of such ultrasonic flow-through cell for continuous roving impregnation is shown in Fig. 6a. Roving and thermoplastic melt were continuously conveyed through the impregnation cavity, treated with ultrasound and extruded through a die to form the final shape of extrudate. Fig. 6b shows a produced continuous fibre-reinforced 3D-printing filament from 24K roving with PLA matrix. This demonstrated the possibility of continuous ultrasound-assisted fibre impregnation without strong decoupling present. The produced 3D-printing filaments showed similar or improved impregnation quality as compared to the results shown in Fig. 2. More details and results of these trials are published in Ref. [29].

5. Conclusions

In this work, the cavitation acoustic pressure and the extension of the cavitation zone were quantified in the PLA melt using a calibrated

cavitometer placed at different locations. Results were then compared with those of water where the cavitation development was apparent. Acoustic spectra analysis revealed that the active cavitation zone in PLA was confined to the 2 mm depth under the tip of the sonotrode.

The measured cavitation field is confined in space, as already in distances of more than 3 mm no cavitation can be detected. Inside the cavitation zone, the characteristic acoustic spectrum is comparable to that of water, but more prominent peaks in the frequency range above 100 kHz are present. This indicates the cavitation bubbles are smaller in size and resonate for longer periods of time. Very strong attenuation but no shielding effects are observed for the PLA melt, in contrast to the acoustic behaviour in water.

This study demonstrated the importance of considering the cavitation phenomena and its spatial distribution in developing continues ultrasound-assisted fibre impregnation processes. Trial results show that high quality fibre impregnation can be achieved within ultrasonic treatment times below 3 s in a continuous process.

Author statement

Iakovos Tzanakis: Funding acquisition, Investigation, Validation, Analysis, Writing- Original draft preparation.

Mohammad Khavari: Software, Writing- Reviewing and Editing.

Maik Titze: Conceptualization, Investigation, Methodology, Analysis, Writing- Reviewing and Editing.

Dmitry Eskin: Funding acquisition, Project administration, Investigation, Writing- Reviewing and Editing.

Declaration of competing interest

The authors declare that they have no known competing financial interests or personal relationships that could have appeared to influence the work reported in this paper.

Acknowledgements

References

[1] Titze M, et al. New technique for impregnating rovings with highly viscous melts. In: ITHEC 2020, 5th International Conference & Exhibition on Thermoplastic Composites. Berlin: ITHEC; 2020.

[2] Liu L, et al. Effect of ultrasound on wettability between aramid fibers and epoxy resin. J Appl Polym Sci 2006;99(6):3172–7.

[3] Khmelev VN, et al. The ultrasonic impregnation of polymer composite materials. In: International conference and seminar of young specialists on micro/nanotechnologies and electron devices. IEEE; 2012. p. 170–3.

[4] Zwinzscher G, Rein S. Ressourcenschonung durch Einsatz eines neuartigen Verfahrens zur Imprägnierung von Verstärkungsfaserstrukturen mit thermoplastischen Matrixmaterialien in kontinuierlichen Prozessen. Chemnitz: Report 32276/01 von der Deutschen Bundesstiftung Umwelt; 2016.

[5] Liu Z, Han Q, Li J. Ultrasound assisted in situ technique for the synthesis of particulate reinforced aluminum matrix composites. Compos B Eng 2011;42(7): 2080–4.

[6] Khandelwal A, et al. Mechanical behavior of AZ31/Al2O3 magnesium alloy nanocomposites prepared using ultrasound assisted stir casting. Compos B Eng 2017;123:64–73.

[7] Matsunaga T, et al. Fabrication of continuous carbon fiber-reinforced aluminum–magnesium alloy composite wires using ultrasonic infiltration method. Compos Appl Sci Manuf 2007;38(8):1902–11.

[8] Qiao J, Li Y, Li L. Ultrasound-assisted 3D printing of continuous fiber-reinforced thermoplastic (FRTP) composites. Additive Manufacturing 2019;30:100926.

[9] Yoon YI, et al. Fabrication of microfibrous and nano-/microfibrous scaffolds: melt and hybrid electrospinning and surface modification of poly (L-lactic acid) with plasticizer. BioMed Res Int 2013;2013:309048. https://doi.org/10.1155/2013/309048.

[10] Chen J, et al. Physical and chemical effects of ultrasound vibration on polymer melt in extrusion. Ultrason Sonochem 2010;17(1):66–71.

[11] Peshkovskii S, et al. Acoustic cavitation and its effect on flow in polymers and filled systems. Polym Compos 1983;4(2):126–34.

[12] Brujan E, Ikeda T, Matsumoto Y. Dynamics of ultrasound-induced cavitation bubbles in non-Newtonian liquids and near a rigid boundary. Phys Fluids 2004;16 (7):2402–10.

[13] Brujan E, et al. Dynamics of laser-induced cavitation bubbles in polymer solutions. Acta Acustica united Acustica 1996;82(3):423–30.

[14] Eskin DG, Tzanakis I. High-Frequency vibration and ultrasonic processing. In: Solidification processing of metallic alloys under external fields. Springer; 2018. p. 153–93.

[15] Lebon GB, et al. Ultrasonic liquid metal processing: the essential role of cavitation bubbles in controlling acoustic streaming. Ultrason Sonochem 2019;55:243–55.

[16] Lebon GB, et al. Numerical modelling of acoustic streaming during the ultrasonic melt treatment of direct-chill (DC) casting. Ultrason Sonochem 2019;54:171–82.

[17] Morton JA, et al. New insights into sono-exfoliation mechanisms of graphite: in situ high-speed imaging studies and acoustic measurements. Mater Today 2021 (in press).

[18] Tzanakis I, et al. In situ observation and analysis of ultrasonic capillary effect in molten aluminium. Ultrason Sonochem 2015;27:72–80.

[19] Tzanakis I, et al. Characterizing the cavitation development and acoustic spectrum in various liquids. Ultrason Sonochem 2017;34:651–62.

[20] Lebon GB, et al. Experimental and numerical investigation of acoustic pressures in different liquids. Ultrason Sonochem 2018;42:411–21.

[21] Khavari M, et al. Characterization of shock waves in power ultrasound. J Fluid Mech 2021;915:R3. https://doi.org/10.1017/jfm.2021.186.

[22] Tzanakis I, et al. Calibration and performance assessment of an innovative high-temperature cavitometer. Sensor Actuator Phys 2016;240:57–69.

[23] Khavari M, et al. Scale up design study on process vessel dimensions for ultrasonic processing of water and liquid aluminium. Ultrason. Sonochem. 2021;76:105647.

[24] Fang Y, Yamamoto T, Komarov S. Cavitation and acoustic streaming generated by different sonotrode tips. Ultrason Sonochem 2018;48:79–87.

[25] Johansen K. Stable-inertial cavitation. PhD Thesis. University of Glasgow; 2018.

[26] Johnston K, et al. Periodic shock-emission from acoustically driven cavitation clouds: a source of the subharmonic signal. Ultrasonics 2014;54(8):2151–8.

[27] Tzanakis I, et al. Characterisation of the ultrasonic acoustic spectrum and pressure field in aluminium melt with an advanced cavitometer. J Mater Process Technol 2016;229:582–6.

[28] Kumar S, Brennen C. Harmonic cascading in bubble clouds. 1992.

[29] Titze M, Kühnast F. Production of continuous fiber-reinforced 3D- printing filaments using ultrasound. In: SAMPE Europe 21 Conference. Baden: SAMPE; 2021.